Vol. 80 (1991) *ACTA PHYSICA POLONICA A* No 2

Proceedings of the XX International School of Semiconducting Compounds, Jaszowiec 1991

FAR-INFRARED MAGNETO-OPTICAL STUDIES OF HgTe-CdTe SUPERLATTICES IN THE SEMIMETALLIC REGIME

T. WOJTOWICZ* , M. DOBROWOLSKA, J.K. FURDYNA

University of Notre Dame, Notre Dame, IN 46556, USA

J.R. MEYER, F.J. BARTOLI, C.A. HOFFMAN

Naval Research Laboratory, Washington, D.C. 20375, USA

AND L.R. RAM-MOHAN

Worcester Polytechnic Institute, Worcester, MA 01609, USA

We review recent magneto-optical investigations performed on HgTe-CdTe semimetallic superlattices. Far infrared magnetotransmission data obtained as a function of temperature, photon energy, and sense of circular polarization are compared with the predictions of a comprehensive new theory which fully incorporates the complexities of type-III superlattice band structure. It is found that the theory accounts for nearly all of the many unusual features which have been observed experimentally. These include the occurrence of two cyclotron resonances due to holes; the coexistence of electron and hole cyclotron resonances in the low temperature limit; the observation of three distinct CRA minima; a step-like change in the temperature dependence of the electron cyclotron mass; and a dramatic increase of the CRI absorption peak intensity with increasing magnetic field.

PACS numbers: 78.65.Fa, 78.30.Fs

*On leave from Institute of Physics, Polish Academy of Sciences, Al. Lotników 32/46, 02–668 Warszawa, Poland.

1. Introduction

HgTe-CdTe superlattices differ from other superlattices in that they consist of alternating layers of a wide-gap and a zero-gap semiconductor. Heterostructures of this type are referred to as type-III superlattices. Since 1979, when the HgTe-CdTe superlattices were first proposed as promising candidates for infrared device applications [1], an intense experimental and theoretical effort has been devoted to the study of these systems. Progress has been particularly rapid during the past four years and good correspondence between band-structure theory and the principal experimental findings has finally emerged. These findings clearly indicate that, while band structure calculations with a small valence-band offset (less than 200 meV) fail to account for the most significant features of the data, the assumption of a large offset (about 350 meV) yields good consistency between theory and experiment [2–7].

Type-III superlattices are said to be semimetallic when electron-like and hole-like bands overlap. The occurrence of such overlap depends on the barrier and well thicknesses and on the temperature [2, 3, 5]. In this article we present a short review of the far-infrared (FIR) magneto-optical properties of semimetallic HgTe-CdTe superlattices. Unless otherwise specified, the data were taken at Notre Dame, using an optically-pumped FIR laser system. The experiments were performed at a series of fixed photon energies in the range between 2.5 and 21.4 meV, in magnetic fields up to 6 T and in the temperature range $1.6 \leq T \leq 200$ K. All data discussed here were obtained in the Faraday geometry ($\boldsymbol{B} \parallel \boldsymbol{k} \parallel \boldsymbol{z}$, where $\boldsymbol{B}$ is the magnetic field, $\boldsymbol{k}$ is the FIR wave vector and $\boldsymbol{z}$ is the superlattice growth direction), using circularly polarized waves. The circular polarization which elicits cyclotron resonance *of electrons* is designated as "cyclotron resonance active" (CRA), and the opposite circular polarization is designated as "cyclotron resonance inactive" (CRI).

Magnetotransmission spectra of semimetallic HgTe-CdTe superlattices are extremely rich in detail [5, 7–9] due to the large number of transition processes which occur in the FIR frequency range. FIR magnetospectroscopy is therefore an especially sensitive and effective tool for probing the very complicated band structure which characterizes type-III superlattices in the semimetallic regime. We show that the current band structure theory of type-III superlattices, along with the assumption of a valence-band offset of 350 meV and careful modeling of the occupation statistics, accounts for nearly all of the wide range of unusual features which have been observed experimentally in these novel and fascinating systems.

2. Band structure of semimetallic superlattice in a magnetic field

In order to illustrate the classes of resonances which may be expected in a typical semimetallic HgTe-CdTe superlattice, we show in Fig. 1 the Landau level scheme as a function of k_z (the wave vector along the growth-direction) for a superlattice with the well and barrier thicknesses $d_W/d_B = 74$ Å/39 Å. The band

structure has been calculated using an 8-band transfer-matrix ($\boldsymbol{k} \cdot \boldsymbol{p}$) algorithm [10], assuming 15% HgTe in the barriers and a valence band offset of 350 meV [2]. In the presence of a magnetic field both the electron-like $E1$ band and the hole-like $HH1$ band are composed of two concurrent series of levels, labeled primed and unprimed, which correspond to the two four-band sets of states discussed for bulk semiconductors by Pidgeon and Brown [11]. In the lowest order, magneto-optical transitions between the primed and the unprimed series are forbidden. The selection rules for the $\sigma^{\pm}$ circular polarizations are $\Delta n = \pm 1$ for both interband and intraband (cyclotron resonance) transitions, where n denotes the Landau level number.

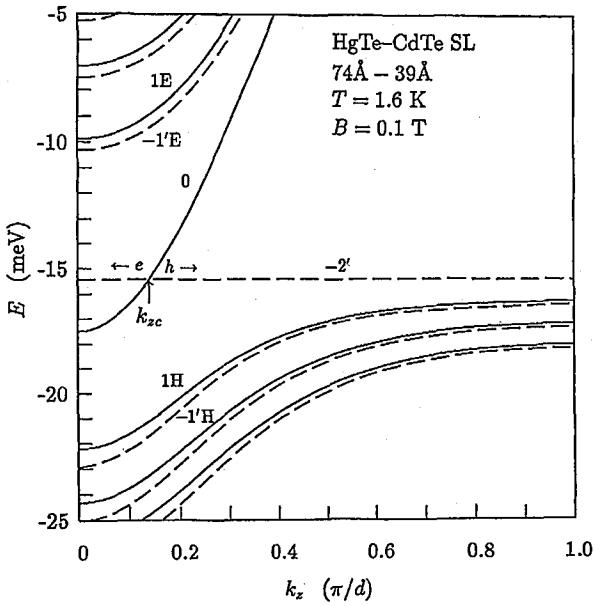

Fig. 1. Landau levels as a function of the wave vector k_z along the growth-direction at $B = 0.1$ T in a [100]-oriented semimetallic HgTe-$Hg_{0.15}Cd_{0.85}Te$ superlattice with $d_W/d_B = 74$ Å/39 Å. Effects of strain are included, and a valence band offset of 350 meV is assumed (reproduced from [13]).

In Fig. 1 all levels above and including $-1'E$ correspond to electron states, while all levels below and including $1H$ are hole states. However, the two levels 0 and $-2'$, which represent the ground states for $E1$ and $HH1$, cross at an intermediate wave-vector k_{zc} and change their character at the crossing point. That is, when $k_z < k_{zc}$, the 0 level belongs to the valence band and $-2'$ to the conduction band, whereas their roles are reversed when $k_z > k_{zc}$. This feature (which makes the superlattice semimetallic) has two important consequences for magneto-optical phenomena. First, because of the overlap of the 0 and $-2'$ levels electrons and holes can coexist in the low-temperature limit, and one may thus expect cyclotron reso-

nances for both CRA and CRI polarizations in the same sample (see discussion in Sections 4.1 and 6, below). Second, since — due to the flatness of the $-2'$ level — electrons and holes can occupy states with a wide range of different k_z, transitions within different portions of the Brillouin zone can now contribute to the total magnetotransmission spectrum. In particular, because of the strong dependence of the hole Landau levels on k_z, two cyclotron resonances due to holes are expected: one at $k_z = 0$ ($1H \rightarrow 0$) and one at $k_z = \pi/d$ ($-1'H \rightarrow -2'$). Furthermore, interband transitions in a semimetallic superlattice can occur in the same spectral range as intraband transitions. Finally, $\Delta n = \pm 1$ transitions originating from different Landau levels have different energies due to the high nonparabolicity of the bands, and can thus yield different absorption peaks.

All these features add significantly to the complexity of magnetotransmission spectra of semimetallic superlattices. In interpreting the observed data, however, one is aided by the fact that, from many transitions which are permitted by the selection rules, only those between an occupied initial state and an unoccupied final state will be observable experimentally. The position of the Fermi level therefore plays a crucial role in determining the relative importance of the various transition processes. In order to identify the features observed experimentally, we calculated the theoretical magneto-optical spectra using a comprehensive new magneto-optical formalism described in detail elsewhere [12]. Up to 70 Landau levels and corresponding matrix elements were calculated as a function of k_z, B, and T. The Fermi level at each temperature and magnetic field was evaluated independently, using the calculated band structure in conjunction with net doping densities obtained from magnetotransport measurements carried on the same samples. The magnetoabsorption coefficient for the Faraday geometry was then obtained for each value of the magnetic field by integrating along k_z over the whole Brillouin zone, and by summing over all allowed transitions.

3. CRI polarization

3. 1. Two cyclotron resonances due to holes

As an example of FIR magnetotransmission for the CRI polarization, we will discuss the data obtained by Perez *et al.* [5] for a p-type semimetallic superlattice with $d_W/d_B = 74$ Å/45 Å. Experimental and theoretical magnetotransmission spectra for this sample at $T = 4.2$ K are illustrated in Fig. 2 for three different FIR photon energies: 5.41, 2.97, and 2.23 meV. The experimental spectra indicate two distinct transmission minima. The theory also predicts two minima, serving to identify the processes involved. The theoretically predicted low-field resonance actually consists of two poorly resolved contributions corresponding to two $k_z = 0$ processes: the interband transition $-1'H \rightarrow -2'$, and the intraband $1H \rightarrow 0$ hole cyclotron resonance. The high-field minimum in the theoretical spectra corresponds to the $-1'H \rightarrow -2'$ hole cyclotron resonance at $k_z = \pi/d$ (see Fig. 1). We thus see that both experimental features occurring in the CRI polarization are due to hole cyclotron resonances originating from different portions of the Brillouin zone.

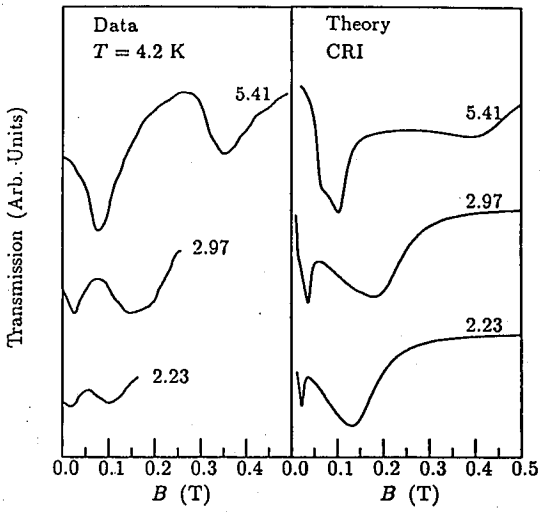

Fig. 2. Experimental (ref. [5]) and theoretical FIR magnetotransmission vs. magnetic field for a p-type HgTe-$Hg_{0.15}Cd_{0.85}Te$ superlattice with nominal $d_W/d_B = 74$ Å/45 Å at $T = 4.2$ K and three different FIR photon energies. In the calculations d_W was adjusted to 78 Å(reproduced from [12]).

We note that the above feature is highly reproducible in type-III structures. For example, two hole cyclotron resonances were consistently observed for other p-type superlattices in our own experiments [12], although the minimum corresponding to the $k_z = \pi/d$ process was somewhat less resolved.

4. CRA polarization

4. 1. Lowest- and higher-order electron cyclotron resonances

The results of our FIR magneto-optical studies of semimetallic HgTe-CdTe superlattices for the CRA polarization are illustrated in Fig. 3 [12]. Although the sample studied was p-type, and the CRI data at $T = 5$ K yielded strong hole cyclotron resonances (similar to those in Fig. 2), weaker resonances were also observed for the CRA polarization at that temperature. The theory predicts that two resolved CRA resonances should be present at low T, one due to the interband process $0 \rightarrow 1E$ (labeled α), the second due to electron cyclotron resonance ($-2' \rightarrow -1'E$, labeled β). The surprising observation of electron cyclotron resonances in a p-type sample in the low-T limit results because (as was discussed in connection with Fig. 1) the $-2'$ level consists of both electron states at small k_z and of hole states at large k_z, all of which are at the same energy. As soon as the magnetic field becomes large enough to accommodate all of the net holes in the $-2'$ ground state, additional holes must be balanced by electrons populating the conduction-band portion of the level (see also discussion in Sec. 6).

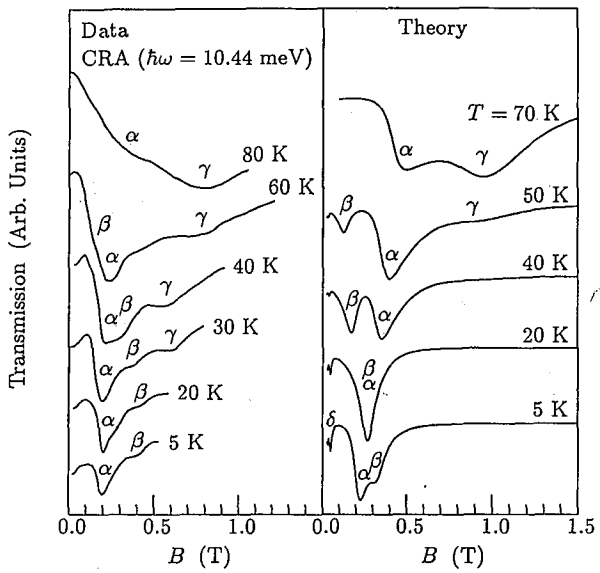

Fig. 3. Experimental and theoretical CRA transmission vs. magnetic field at several temperatures for a p-type HgTe-$Hg_{0.15}Cd_{0.85}$Te superlattice, for $\hbar\omega = 10.44$ meV. α refers to the $0 \rightarrow 1E$ transition, β to $-2' \rightarrow -1'E$, γ is a combination of higher-order electron cyclotron resonance transitions ($1E \rightarrow 2E$, $-1'E \rightarrow 0'E$, etc.), and δ refers to the first two higher-order interband transitions ($1H \rightarrow 2E$ and $-1'H \rightarrow 0'E$). Nominal d_W/d_B values for the superlattice were 64 Å/40 Å. In the calculations, the value of d_W had to be adjusted to 74 Å to obtain the semimetallic behavior, as discussed in [12] from which the figure is taken.

When the temperature is increased above 5 K, two principal qualitative trends are observed. First, the minima become stronger due to the thermal generation of additional electrons. Second, the β resonance at 10.44 meV moves to lower magnetic fields, first approaching the α minimum, and then crossing it. It should be noted here that the level marked in Fig. 1 moves up relative to $-2'$, and may eventually rise above it [12]. When this happens, we have a semimetal-to-semiconductor transition. The temperature at which the resonant fields of the α and β minima coincide corresponds very nearly to this semimetal-to-semiconductor transition of the superlattice. For temperatures above the transition the 0 level lies above $-2'$ at $k_z = 0$ and becomes the conduction-band ground state for all k_z . This reverses the interpretations of the two minima, i.e., α ($0 \rightarrow 1E$) becomes a cyclotron resonance process, while β ($-2' \rightarrow -1'E$) becomes an interband resonance. Figure 3 shows that, although the semimetal-to-semiconductor transition occurs near 40 K in the experimental spectra and at 20 K in the theory, the qualitative behaviour is quite similar in the two cases.

At temperatures above 30 K the experimental spectra show the appearance of a third resonance, labeled γ. This feature grows rapidly with temperature, and

eventually dominates the entire spectrum. The theory accurately reproduces this feature, and identifies it as the collective effect of higher-order electron cyclotron resonance transitions (those involving $1E \rightarrow 2E$, $-1'E \rightarrow 0'E$, etc.). Considering the many processes involved, the overall agreement between the experimental and theoretical spectra is seen to be remarkably good.

4.2. Further effects of higher order cyclotron resonances

The temperature dependence of the cyclotron effective mass of electrons is plotted in Fig. 4 using data from Fig. 3. Results for both the α and γ minima are shown, with α minima given only at temperatures for which the feature may be interpreted as a cyclotron resonance rather than an interband process ($T >$ 40 K for the experiment, $T >$ 20 K for the theory). The theory predicts that

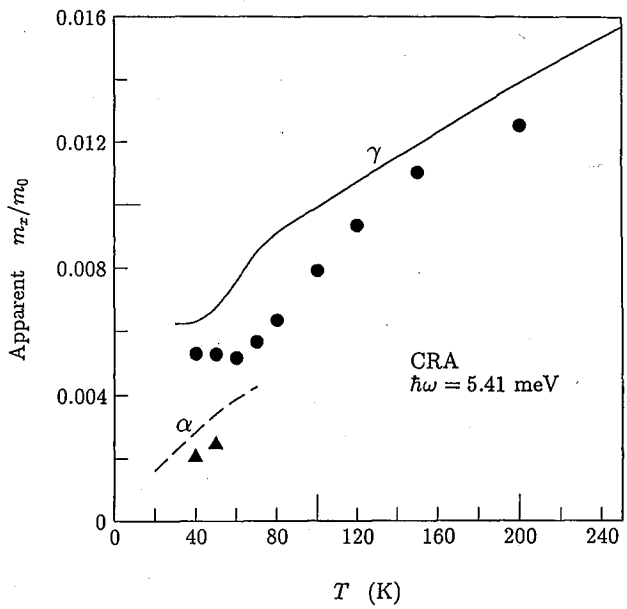

Fig. 4. Experimental (points) and theoretical (curves) electron cyclotron mass vs temperature corresponding to the data of Fig. 3 at $\hbar\omega = 5.41$ meV (reproduced from [12]).

cyclotron resonance energies for the first two higher-order transitions ($1E \rightarrow 2E$ and $-1'E \rightarrow 0'E$) are nearly independent of T. As long as these processes dominate the γ minimum, $m_x^\gamma(T)$ is relatively flat. However, at temperatures above 40 K higher-order excited processes ($0'E \rightarrow 1'E$, $2E \rightarrow 3E$, etc.) are expected to become important, and m_x^γ begins to increase. Higher temperatures lead to contributions from still higher orders, hence the mass continues to increase. This is essentially a nonparabolicity effect. Although the abrupt step in the slope of the experimental $m_x^\gamma(T)$ occurs at 60 K rather than 40 K, as predicted by the theory, the two

temperature dependences are qualitatively quite similar. The experimental and theoretical results for the α minimum are also seen to be in reasonable agreement: the theory predicts an increase of m_x^α with temperature due to the increase of the energy gap with T, and such an increase is seen experimentally, at least in the limited data available.

5. Magnetic activation of a bipolar plasma

The band structure of semimetallic HgTe-CdTe superlattices discussed in Sec. 2 has another consequence which is — to our knowledge — unique in solid state physics: the magnetic activation of a bipolar (electron and hole) plasma, whose density increases with field when B exceeds a certain critical value, B_{crit}.

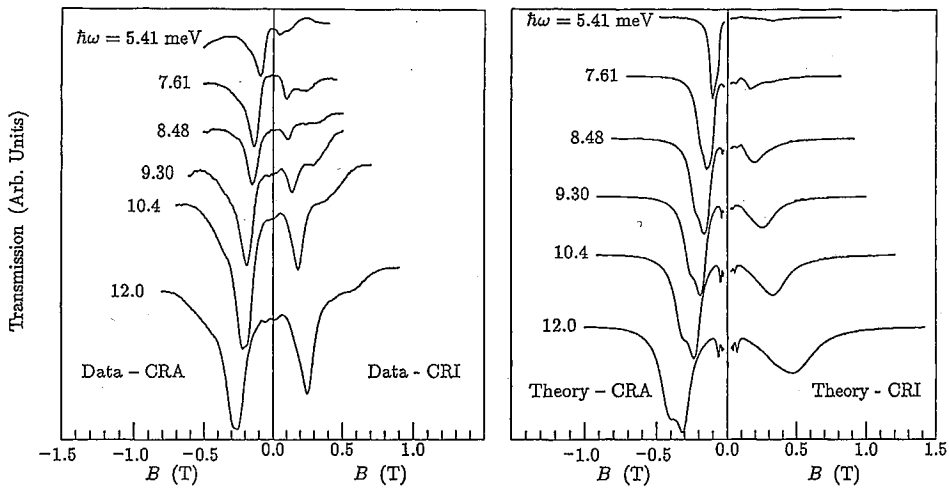

Fig. 5. Experimental and theoretical CRA and CRI transmission vs. magnetic field at $T = 1.6$ K for six different FIR photon energies. Experiment was performed on a HgTe-$Hg_{0.15}Cd_{0.85}Te$ superlattice with nominal values $d_W/d_B = 75$ Å/36 Å grown on a [211] CdTe substrate. The calculations assume $N_D - N_A = 6 \times 10^{14}$ cm^{-3}, other parameters being the same as those used in the calculation for Fig. 1 (reproduced from [13]).

The left-hand side of Fig. 5 shows experimental magnetotransmission spectra taken at $T = 1.6$ K for a n-type superlattice with $d_W/d_B = 74$ Å/36 Å [13]. The CRA spectra for all 6 photon energies are dominated by a strong cyclotron resonance minimum. In contrast, the structure in the CRI spectrum for the lowest $\hbar\omega$ (5.41 meV) is barely discernible. However, with increasing frequency the low-field CRI absorption peak grows rapidly, until at 12.0 meV its magnitude is nearly as large as that of the CRA resonance. This abrupt emergence of the CRI resonance is ascribed to the activation of minority holes when the magnetic field reaches a critical value (see below). The "critical" nature of the process is evident from the abruptness

of the increase of CRI absorption at photon energies near 8 meV, i.e. when the magnetic field at resonance reaches the field of ~ 0.15 T. In order to verify that these observations are in agreement with the behavior expected when minority holes are magnetically activated, in the right-hand side of Fig. 5 we present the theoretical magnetotransmission for a superlattice with $N_D - N_A = 6 \times 10^{14}$ cm^{-3}. Although the calculated CRI resonance is somewhat broader than in the data, we find that the main features of the two spectra are in excellent agreement: while the CRA minimum is strong at all photon energies, the theory predicts a negligible absorption of the CRI-polarized radiation until the resonance field approaches the critical value, as is indeed observed experimentally.

This effect can be qualitatively understood on the basis of the band structure illustrated in Fig. 1. In the low-field limit, E_F for a n-type superlattice must lie above many Landau levels in the conduction band, since the density of states per level is proportional to B. However, since fewer levels are required as the field is increased, one eventually reaches a critical field B_{crit} at which the density of states in the $-2'$ level is large enough to accommodate the entire electron population. If one then increases the field beyond this critical value, the electron portion of $-2'$ becomes *partially* unoccupied, because the density of states is greater than that required by the electrons. However, this automatically implies that the hole portion of that level must be partially occupied, since the electron and hole portions are at the same energy. Electrons and holes therefore coexist in the zero-temperature limit whenever $B > B_{crit}$, and the concentration of such a field-induced bipolar plasma increases roughly linearly with $(B - B_{crit})$.

6. Conclusions

In this article we presented several examples of new phenomena observed in recent FIR magneto-optical studies of semimetallic HgTe-CdTe superlattices. The FIR magneto-optical spectra of HgTe-CdTe superlattices are quite complex, due to the large number of possible processes which can contribute distinct resonances within the FIR spectral range. For an unambiguous interpretation of such complex data it was crucial to carry out the experiments over a broad range of temperature and photon energy, using both CRI and CRA polarizations .

We have demonstrated that, by fully accounting for the details of the unique band structure of semimetallic HgTe-CdTe superlattice and by carefully modeling the occupation statistics, we are able to account for nearly all of the wide range of unusual features in the data. These include the presence of two types of cyclotron resonances due to holes; the coexistence of both electron and hole cyclotron resonances in the low temperature limit in p-type specimens; the simultaneous observation of three distinct CRA minima due to interband transitions, lowest-order intraband transitions, and higher-order intraband transitions; a sudden change in the electron cyclotron mass as a function of temperature; and a dramatic increase in n-type superlattices of the intensity of a CRI absorption peak with increasing magnetic field due to the magnetic activation of minority carriers.

The good qualitative — and in many cases also quantitative — agreement between experiment and theory can be seen as a positive test of the current band

structure theory of type-III superlattices, and as an additional confirmation of the large valence band offset between HgTe and CdTe [2]. The results presented also demonstrate that FIR magneto-optical measurements constitute a very effective and powerful tool for band structure studies of narrow gap superlattices.

Acknowledgments

One of the authors (T. W.) would like to thank the University of Notre Dame for the hospitality extended to him during his stay there. The work at Notre Dame was supported by NSF grant DMR8904802. The work at NRL was supported in part by the Office of Naval Research and in part by SDIO/IST.

References

[1] J.N. Schulman, T.C. McGill, *Appl. Phys. Lett.* **34**, 663 (1979).

[2] For a recent review see:
J.R. Meyer, C.A. Hoffman, F.J. Bartoli, *Semicond. Sci. Technol.* **5**, S90 (1990);
J.P. Faurie, *IEEE J. Quantum Electron.* **QE-22**, 1656 (1986);
T.C. McGill, G.Y. Wu, S.R. Hetzler, *J. Vac. Sci. Technol. A* **4**, 2091 (1986).

[3] C.A. Hoffman, J.R. Meyer, F.J. Bartoli, J.W. Han, J.W. Cook Jr., J.F. Schetzina, J.N. Schulman, *Phys. Rev. B* **39**, 5208 (1989).

[4] N.F. Johnson, P.M. Hui, H. Ehrenreich, *Phys. Rev. Lett.* **61**, 1993 (1988).

[5] J.M. Perez, R.J. Wagner, J.R. Meyer, J.W. Han, J.W. Cook Jr., J.F. Schetzina, *Phys. Rev. Lett.* **61**, 2261 (1988).

[6] J.N. Schulman, O.K. Wu, E.A. Patten, J.W. Han, Y. Lansari, L.S. Kim, J.W. Cook Jr., J.F. Schetzina, *Appl. Phys. Lett.* **53**, 2420 (1988).

[7] J.M. Berroir, Y. Guldner, J.P. Vieren, M. Voos, X. Chu, J.P. Faurie, *Phys. Rev. Lett.* **62**, 2024 (1989).

[8] C.A. Hoffman, J.R. Meyer, R.J. Wagner, F.J. Bartoli, X. Chu, J.P. Faurie, L.R. Ram-Mohan, H. Xie, *J. Vac. Sci. Technol. A* **8**, 1200 (1990).

[9] M. Dobrowolska, T. Wojtowicz, H. Luo, J.K. Furdyna, O.K. Wu, J.N. Schulman, J.R. Meyer, C.A. Hoffman, F.J. Bartoli, *Phys. Rev. B* **41**, 5084 (1990).

[10] L.R. Ram-Mohan, K.H. Yoo, R.L. Aggarwal, *Phys. Rev. B* **38**, 6151 (1988).

[11] C.R. Pidgeon, R.N. Brown, *Phys. Rev.* **146**, 575 (1966).

[12] J.R. Meyer, R.J. Wagner, F.J. Bartoli, C.A. Hoffman, M. Dobrowolska, T. Wojtowicz, J.K. Furdyna, L.R. Ram-Mohan, *Phys. Rev. B* **42**, 9050 (1990).

[13] J.R. Meyer, C.A. Hoffman, F.J. Bartoli, T. Wojtowicz, M. Dobrowolska, J.K. Furdyna, X. Chu, J.P. Faurie, L.R. Ram-Mohan, to be published.